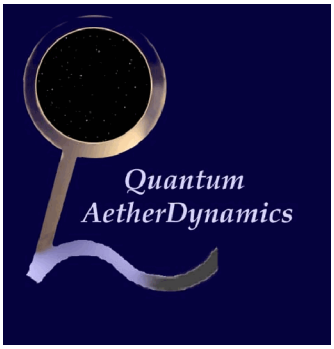

Quantum AetherDynamics Institute (QADI)

Casimir Boundary Stress in the Aether Physics Model (APM): Ontology, QMU Quantification, Coefficient Anatomy, and Experimental Discriminators

David W. Thomson III
Quantum AetherDynamics Institute (QADI), Alma, Illinois, USA
ORCID: 0000-0002-5830-5427

Version 1.1 – September 10, 2026

This article is published by the Quantum AetherDynamics Institute (QADI).

It develops the Aether Physics Model (APM)

Abstract

This paper is a ledger-first compendium of the Aether Physics Model (APM) interpretation of the Casimir effect in Quantum Measurement Units (QMU). Casimir attraction is treated as *boundary-induced Aether stress*: distributed-charge boundary ensembles impose geometric constraints on the Aether substrate, producing curvature loading carried by the QMU quantity *curl* and closing through $A_u \cdot \mathrm{curl} = {F_q}^2 {\lambda_C}^2$. The conventional ideal parallel-plate law is translated into QMU using $\mathrm{phtn} = m_\mathrm{e} {\lambda_C}^3 {F_q}^2$, while the APM ideal-limit proposal is kept separate: $C_\mathrm{APM} = 1/(16\pi^2)$ versus $C_\mathrm{Casimir} = \pi/480$ in the h-based convention. Version 1.1 removes the obsolete interpretation of the algebraic ratio $\pi^3/30$ as an APM "inventory factor." That ratio has no independent physical status in the present APM formulation. Material, geometry, thermal, roughness, and patch-potential corrections remain necessary for comparison with real experiments, but they may not be used as a free residual multiplier that renormalizes the protected APM ideal coefficient into the conventional value. A QMU-first experimental program is specified to extract an ideal-limit dimensionless coefficient with quantified systematics and thereby discriminate the two predictions.

Keywords: QMU; APM; Casimir; Aether ontology; chronovibration; magnetic charge; holonomy; β_0; phtn; A_u; coefficient metrology

1 Scope and deliverables

This document is written to end recurring debates about "what is physically happening" in Casimir physics and "which numerical coefficient is exact." It provides:

1. APM ontology of vacuum dynamics (what exists and what is dynamic).
2. A ledger-first QMU quantification of the parallel-plate Casimir law.
3. A clean comparison of the APM ideal coefficient $1/(16\pi^2)$ with the conventional ideal coefficient $\pi/480$, without assigning physical meaning to their algebraic ratio.
4. Interfaces to prior QADI work: Unified Force Theory (magnetic charge bridge), Casimir–Nuclear Chronovibration (boundary ensembles and coherence), photoelectric action transfer, and universal $1/(16\pi^2)$ appearances at cosmic scale.
5. A falsifiable experimental compendium designed to discriminate the protected APM ideal coefficient from the conventional ideal coefficient after independently constrained real-material corrections.

2 Symbols, units, and operational definitions

This section is included explicitly to prevent notation drift and to keep bookkeeping from becoming reified. All quantities are QMU-native; no SI conversion is required to use this paper as a laboratory reference.

Symbol	QMU name	Definition (ledger form)	Operational meaning / how it is used here
m_{e}	electron mass	base atom	mass unit for matter quanta and action unit construction.
λ_C	quantum length	base atom	quantum cell length; sets dimensionless geometry $\hat{a} = a/\lambda_C$ and $\hat{A} = A/{\lambda_C}^2$.
F_q	quantum frequency	base atom	chronovibration tick; appears in Ledger One closure.
phtn	photon action	phtn $= m_{\mathrm{e}}\,{\lambda_C}^3 {F_q}^2$	action-transfer quantum; used to write Casimir pressure without $\hbar$.
A_u	Aether unit	base atom	Aether stiffness/rotational modulus in Ledger One.
curl	curl	base atom	curvature/torsion operator carrying boundary loading; closes with A_u via Ledger One.
k_C	Coulomb constant	base atom	charge-geometry coupling constant; appears in the magnetic-charge bridge.
${e_{\mathrm{emax}}}^2$	magnetic charge	base atom	distributed magnetic charge; Casimir reframed as $k_C {e_{\mathrm{emax}}}^2$ channel.
$16\pi^2$	Aether modulus ratio	$16\pi^2 = A_u/k_C = 16\pi^2$	universal geometry modulus ratio; defines holonomy quotient β_0.
β_0	Aether geometry quotient	$\beta_0 = 1/(16\pi^2)$	protected APM ideal-limit coefficient proposed for the parallel-plate boundary law.
C	normalized plate coefficient	$C \equiv -(F/A)a^4/\mathrm{phtn}$	dimensionless coefficient inferred after independently constrained corrections; compare C_{APM} and C_{Casimir}.
ξ_B	boundary coherence	defined in chronovibration work	participation/coherence knob for boundary ensembles in APM-specific tests.
Σ_B^b	surface inventory	defined in chronovibration work	boundary inventory density parameter used in ensemble channel normalization.
κ	coherence (phase lock)	defined in chronovibration work	global phase alignment parameter for chronovibration response.

Table 1: Ledger-first symbol table for this paper. "base atom" indicates a primitive QMU constant defined by the QADI class/macros; composite definitions are given where used.

Primary reporting recommendation. When presenting experimental results derived from this paper, report the extracted coefficient as

$$C(\hat{a}) \quad \text{with} \quad \text{systematic controls and an uncertainty budget,}$$

not merely a force value at one separation.

3 APM ontology axioms for vacuum stress

This section states the physical commitments used later. It is not philosophical decoration; it fixes what counts as a cause.

3.1 Axiom A: quantized Aether substrate with chronovibration

Space is a structured, quantized Aether medium composed of discrete Aether units. Its primitive time-like degree of freedom is chronovibration at invariant frequency F_q. Coherence does not alter F_q; it alters phase alignment, parameterized by $\kappa \in (0, 1]$ and boundary coherence factors such as ξ_B Thomson III [2025a].

3.2 Axiom B: two charges (electrostatic and magnetic), both distributed

APM distinguishes electrostatic charge e^2 and magnetic (electromagnetic/strong) charge ${e_{\text{emax}}}^2$. Both are treated as distributed (squared) quantities; geometry is intrinsic to charge. This is the basis for reading condensed-matter quantization (e.g., Hall and Josephson chains) as charge-geometry metrology rather than as abstract constants Thomson III and Bourassa [2025].

3.3 Axiom C: photons are action-transfer quanta

In APM a photon unit phtn is an action-transfer quantum,

$$\text{phtn} \equiv m_{\text{e}}\, {\lambda_C}^3 {F_q}^2. \tag{1}$$

Light propagates continuously but couples discretely via action transfer. This framing is consistent with QADI photoelectric analysis in which emission and absorption are angular-momentum transfer processes rather than "particles in transit" descriptions Thomson III [2025d].

3.4 Axiom D: boundaries convert geometry into stress

Conducting boundaries are distributed-charge ensembles that impose geometric constraints on nearby Aether units. Casimir force is the mechanical manifestation of the resulting Aether stress gradient.

4 Ledger closure and universal geometry

4.1 Ledger One: Aether rotational self-identity

Ledger One (standardized QADI format) is

$$A_u \cdot \mathrm{curl} = {F_q}^2 {\lambda_C}^2. \tag{2}$$

It closes Aether stiffness A_u with curvature (curl) and chronovibrational propagation ${F_q}^2{\lambda_C}^2$. This identity is the ledger mechanism by which boundary curvature becomes measurable stress.

4.2 Universal modulus ratio and holonomy quotient

APM fixes a canonical electromagnetic Aether modulus ratio

$$\frac{A_u}{k_C} = 16\pi^2, \tag{3}$$

so the reciprocal

$$\beta_0 \equiv \frac{1}{16\pi^2} \tag{4}$$

is a universal Aether geometry (holonomy) quotient. QADI work on cosmic polarization rotation predicts β_0 as a parameter-free topology quotient, motivating its interpretation as universal rather than Casimir-specific Thomson III [2025c].

5 Casimir boundary geometry in QMU

5.1 Dimensionless geometry

For two parallel boundaries separated by a with projected area A, define

$$a = \hat{a}\,\lambda_C, \qquad A = \hat{A}\,{\lambda_C}^2. \tag{5}$$

All geometry dependence becomes dimensionless in $(\hat{a}, \hat{A})$.

5.2 Parallel-plate force law in QMU

Casimir derived the ideal parallel-plate law for perfectly conducting plates by evaluating the boundary-imposed mode inventory in the gap Casimir [1948]. Write the parallel-plate Casimir force as

$$F_C \;=\; -\frac{\pi}{480}\,\mathrm{phtn}\,\frac{A}{a^4} \;=\; -\frac{\pi}{480}\,\frac{\mathrm{phtn}}{{\lambda_C}^2}\,\frac{\hat{A}}{\hat{a}^4}. \tag{6}$$

This is the familiar ideal coefficient expressed in the phtn convention (i.e., h rather than $\hbar$ bookkeeping). At the quantum cell $(\hat{A}, \hat{a}) = (1, 1)$,

$$F_{C,\mathrm{cell}} \;=\; -\frac{\pi}{480}\,\frac{\mathrm{phtn}}{{\lambda_C}^2}. \tag{7}$$

6 Coefficient anatomy: two competing ideal predictions

This section records the Version 1.1 correction. The conventional and APM coefficients are not factors in one physical formula; they are competing ideal-limit predictions.

6.1 Conventional ideal coefficient

Casimir's 1948 result is commonly written with $\hbar$ as $\pi^2/240$ in the pressure law Casimir [1948]. Since $\hbar = h/(2\pi)$, the same ideal result in the h (and therefore phtn) convention is

$$C_{\text{Casimir}} = \frac{\pi}{480} \approx 6.544985 \times 10^{-3}. \tag{8}$$

This conversion changes notation, not physics.

6.2 APM ideal coefficient

The APM geometric modulus ratio is $A_u/k_C = 16\pi^2$, with reciprocal quotient

$$C_{\text{APM}} = \frac{k_C}{A_u} = \frac{1}{16\pi^2} \approx 6.332574 \times 10^{-3}. \tag{9}$$

In the present formulation this quotient is the proposed APM normalization of the ideal parallel-boundary stress. The explicit Aether two-boundary calculation that must recover both the a^{-4} dependence and this normalization remains a separate dynamical task; the coefficient is therefore a protected, falsifiable APM proposal rather than an empirical fit.

6.3 The ratio $\pi^3/30$ has no independent APM ontology

Algebraically,

$$\frac{C_{\text{Casimir}}}{C_{\text{APM}}} = \frac{\pi^3}{30} \approx 1.03354. \tag{10}$$

Equation (10) is only the ratio of the two predictions. Version 1.1 explicitly withdraws the earlier interpretation of $\pi^3/30$ as an electromagnetic inventory, holonomy correction, participation factor, or other physical APM quantity. No such independent factor has been derived. The conventional coefficient is approximately 3.35% above the APM coefficient when normalized to C_{APM}.

6.4 Protected prediction and real-material corrections

For the ideal parallel-boundary limit the two hypotheses are

$$H_A:\ C = \frac{1}{16\pi^2}, \qquad H_C:\ C = \frac{\pi}{480}. \tag{11}$$

Real experiments require independently justified corrections for finite conductivity and dielectric response, temperature, roughness, geometry, calibration, and patch potentials. Such corrections map a real apparatus toward an ideal-limit coefficient; they are not a free multiplier on Eq. (9). No residual parameter may be introduced merely to slide $1/(16\pi^2)$ toward $\pi/480$. If controlled ideal-limit inference excludes Eq. (9), the APM Casimir normalization fails.

7 Magnetic-charge reframing of the APM proposal

A key APM bridge is

$$\frac{\text{phtn}}{16\pi^2} = k_C \, {e_{\text{emax}}}^2. \tag{12}$$

Thus the protected APM ideal-limit proposal may be written

$$\frac{F_C^{\text{APM}}}{A} = -\frac{1}{16\pi^2}\frac{\text{phtn}}{a^4} = -\frac{k_C {e_{\text{emax}}}^2}{{\lambda_C}^2}\left(\frac{\lambda_C}{a}\right)^4. \tag{13}$$

This is the coefficient-level APM prediction to be tested. It must not be multiplied by $\pi^3/30$ or by an unconstrained participation factor to reproduce the conventional ideal result.

8 Connection to boundary-ensemble chronovibration formulation

The Casimir–Nuclear Chronovibration paper treats Casimir boundaries as an ensemble channel that contributes to Aether load through coherence κ and boundary inventory parameters (dimensionless spacing $\hat{a}$, surface inventory Σ_B^b, boundary coherence ξ_B) Thomson III [2025a]. The key practical mapping is:

1. The two-body plate law constrains the normalized coefficient C through a^{-4} scaling and geometry normalization.
2. The ensemble channel constrains inventory and participation through $\hat{a}^{-3}$ scaling once boundary density is volume-normalized.

A boundary-array experiment can therefore constrain the two-body coefficient C while separately probing ensemble participation parameters used in chronovibration work. Those participation parameters are not correction factors for the protected ideal coefficient.

9 Casimir-driven Aether nucleation (ontology extension)

This section imports the minimum necessary ontology extension from the Zenodo record on Casimir-driven nucleation, while preserving this paper's role as a coefficient-and-ontology reference. The purpose is to connect static Casimir stress to an explicit APM micro-process (nucleation / unit-creation), without requiring any Standard Model vacuum-field language.

9.1 Mechanism statement (claim)

Casimir boundary loading can drive nucleation of new Aether units when the interacting boundaries achieve chronovibrational alignment at a Compton-wavelength separation Thomson III [2025b]. In this statement, the physical "cause" is not an abstract field fluctuation; it is the boundary-conditioned Aether stress state crossing a nucleation criterion under phase-lock alignment.

9.2 Formal anchor (interface)

The mechanism is posed in the Zenodo record as a Lagrangian formulation in QMU, intended to provide a single dynamical spine that connects boundary loading, coherence/phase variables, and creation thresholds Thomson III [2025b]. In this compendium, that formalism is treated as the *dynamical backend* for two uses: (i) a micro-process vocabulary for what happens under boundary stress, and (ii) a future-proof interface for extending coefficient work into threshold work without rewriting the ontology each time.

9.3 Scope bridge (closure chain interface)

The Zenodo record explicitly ties the framework to atomic electron binding energies and to a first-principles nuclear binding functional Thomson III [2025b]. This is critical for compendium completeness: it ensures Casimir ontology is not standalone. Instead, Casimir boundary stress becomes one metrological and dynamical portal into the same closure chain that also constrains atomic binding and nuclear pairing.

9.4 How this strengthens the compendium

This ontology extension gives the reader a single, explicit "what happens physically" answer in APM terms (nucleation/unit-creation under boundary-conditioned Aether stress), rather than stopping at coefficient anatomy. Operationally, it also justifies why coherence-modulated Casimir tests belong in the same foundational reference paper as the coefficient extraction SOP: the same experimental knobs can probe both the normalized Casimir coefficient C and nucleation thresholds.

9.5 Collider ontology and rupture threshold as a boundary-defect analogue

The same record provides a concrete extension of boundary ontology: "quark/gluon" phenomenology is treated as observable boundary defects on Aether units, with a falsifiable rupture threshold for break-apart conditions Thomson III [2025b]. For compendium use, the import is deliberately narrow:

1. **Mapping (claim):** boundary defect spectrum $\leftrightarrow$ rupture threshold. The "spectrum" is the class of defect signatures; the "threshold" is the stress/coherence condition at which units rupture or reorganize.
2. **Falsifiability spine:** the rupture threshold is testable, and therefore belongs in the same falsifiability spine as the Casimir coefficient C rather than as speculative color. In practice, it introduces an additional measured parameter (a nucleation/rupture threshold) that can be correlated with boundary conditioning and geometry.

10 Experimental compendium: decisive tests of the normalized coefficient

This section integrates tests into the foundational ontology; it is not an afterthought.

10.1 What "exact" means operationally

A coefficient determination is definitive only if C is:

1. separation-invariant across a controlled range in $\hat{a}$,
2. geometry-invariant across at least two configurations, and
3. stable under explicit modeling or cancellation of systematics (patch potentials, roughness, finite conductivity, temperature/thermal response).

The experimental target is not "a force at one distance" but a robust estimate of C with a transparent uncertainty budget.

10.2 Primary discriminators (recommended sequence)

1. **Baseline replication and scaling check (historical anchor).** Replicate a torsion-pendulum or equivalent baseline measurement across a decade of separations and verify a^{-4} scaling stability as a prerequisite to coefficient work Lamoreaux [1997].
2. **Differential/isoelectronic Casimir.** Use composition sectors under a common overlayer to suppress patch contributions and isolate subtle coefficient structure. This class of measurement is motivated as a route to improved robustness against patch systematics and improved sensitivity to low-frequency/thermal contributions Bimonte et al. [2016].
3. **Patch-characterized force (in situ potential diagnostics).** Combine force measurement with surface potential mapping so the patch spectrum is measured rather than assumed. Patch systematics have been shown to dominate the interpretation of several precision configurations and must be explicitly closed for coefficient claims Sushkov et al. [2011].
4. **Precision coefficient extraction with controlled systematics.** High-precision configurations with detailed modeling provide strong constraints and are valuable for establishing whether $C(\hat{a})$ is separation-invariant once corrections are applied Decca et al. [2005].
5. **Geometry cross-check: normal and lateral channels.** Measure a second geometry class (e.g., lateral Casimir in corrugated boundaries) so C is not inferred through a single mapping approximation.
6. **Temperature knob.** Repeat a coefficient extraction at multiple temperatures so thermal corrections do not masquerade as a different C.
7. **APM-specific coherence modulation.** At fixed $\hat{a}$, modulate boundary coherence/conditioning (raising ξ_B) and test for reversible shifts in the measured coefficient C. A reproducible, monotone dependence of the measured coefficient C on coherence would support participation-dependent Aether stress rather than an immutable ideal-inventory constant; in the nucleation ontology, this additionally probes whether boundary stress can cross a coherence threshold for Aether-unit creation Thomson III [2025b].

10.3 QMU-first coefficient extraction recipe

For pressure $P = F/A$, define

$$C(a) = -P(a)\frac{a^4}{\text{phtn}}. \tag{14}$$

After independently constrained corrections for known apparatus and material effects, examine whether $C(a)$ approaches a separation-invariant ideal-limit value. The discriminating targets are Eqs. (9) and (8); no inventory or residual multiplier is fitted between them.

10.4 Decision logic

- If the corrected ideal-limit coefficient approaches $C_{\text{Casimir}} = \pi/480$, the conventional ideal normalization is supported over the APM normalization.
- If it approaches $C_{\text{APM}} = 1/(16\pi^2)$, the APM ideal normalization is supported.
- If it approaches neither value, neither ideal coefficient is established by that dataset; residual systematics or a different physical model must be investigated without introducing an ad hoc multiplier into the APM prediction.

11 Conclusions

Casimir attraction is quantified in APM as boundary-induced Aether stress in QMU. Version 1.1 makes a substantive coefficient correction: the conventional ideal value $\pi/480$ and the APM value $1/(16\pi^2)$ are treated as competing ideal-limit predictions, not as factors in one coefficient anatomy. The identity $C_{\text{Casimir}}/C_{\text{APM}} = \pi^3/30$ is retained only as an algebraic comparison; its former interpretation as an APM inventory or holonomy/participation factor is withdrawn. The APM prediction is protected: ordinary real-material and apparatus corrections may be applied when independently measured or modeled, but no free residual multiplier may renormalize $1/(16\pi^2)$ into the conventional value. The experimental program therefore has a simple objective: infer the ideal-limit dimensionless coefficient with uncertainty comfortably below the approximately 3.35% separation and determine which, if either, prediction survives. The separate Casimir-driven nucleation sector remains an APM ontology extension and may motivate coherence or threshold experiments, but its participation variables are not coefficient-repair parameters.

A Coefficient-extraction SOP for a decisive experiment

This appendix gives a compact procedure for comparing experiment with the two protected ideal hypotheses without reintroducing the obsolete inventory factor.

A.1 Required inputs

For each data point record separation a_i, force F_i, effective interaction area A_i where applicable, temperature, surface preparation, calibration state, and independently measured or modeled corrections for electrostatic patches, roughness, finite conductivity/dielectric response, and geometry.

A.2 Raw normalized coefficient

For a parallel-plate pressure $P_i = F_i/A_i$, compute

$$C_i^{\mathrm{raw}} = -P_i \frac{a_i^4}{\mathrm{phtn}}. \tag{15}$$

Apply only corrections supported by independent measurements or a specified material/geometry model, then report corrected C_i and its uncertainty budget. Do not fit a free multiplicative factor whose purpose is to move the result toward either target coefficient.

A.3 Acceptance criteria

A dataset is suitable for coefficient discrimination only when the inferred ideal-limit coefficient is stable across a nontrivial separation range, repeatable under unchanged conditioning, robust to controlled variation of known systematics, and cross-checked in at least one independent geometry or experimental configuration. Report

$$C = \bar{C} \pm \sigma_{\mathrm{stat}} \pm \sigma_{\mathrm{sys}}, \tag{16}$$

with systematic contributions broken out at minimum into separation calibration, effective area or geometry mapping, patch potential uncertainty, roughness, finite conductivity/dielectric response, and temperature where relevant.

A.4 Decision rules

The ideal targets are

$$C_{\mathrm{APM}} = \frac{1}{16\pi^2}, \qquad C_{\mathrm{Casimir}} = \frac{\pi}{480}. \tag{17}$$

If the corrected ideal-limit result excludes one target while remaining compatible with the other, the experiment discriminates the two normalizations. If both are excluded, neither hypothesis is rescued by defining a new APM inventory or holonomy factor.

A.5 Recommended experimental sequence

1. Reproduce the separation dependence and calibration in a baseline configuration Lamoreaux [1997].
2. Use differential or isoelectronic designs where useful to suppress patch-related ambiguity Bimonte et al. [2016].
3. Characterize surface potentials and other electrostatic backgrounds rather than absorbing them into the Casimir coefficient Sushkov et al. [2011].
4. Use precision force measurements with explicit material and thermal corrections Decca et al. [2005].
5. Cross-check at least one independent geometry and, where practical, more than one temperature.
6. Treat APM-specific coherence or nucleation tests as separate observables. A reproducible coherence dependence would be new physics to model; it is not a license to renormalize C_{APM}.

B Version 1.1 correction record

Version 1.0 defined $I_C = \pi^3/30$ as an "ideal EM inventory factor" and introduced a correction parameter H_C. Version 1.1 withdraws both physical interpretations. The exact algebraic identity

$$\frac{\pi/480}{1/(16\pi^2)} = \frac{\pi^3}{30} \tag{18}$$

remains true, but the right-hand side is only the ratio of the conventional and APM ideal predictions. It is not an independently derived APM quantity. The protected APM ideal coefficient is $1/(16\pi^2)$.

Acknowledgments

QADI publications and data are archived with DOIs in the AetherPhysics Zenodo community.

References

G. Bimonte, D. López, and R. S. Decca. Isoelectronic determination of the thermal casimir force. *Physical Review B*, 93(18):184434, 2016. doi: 10.1103/PhysRevB.93.184434. URL https://doi.org/10.1103/PhysRevB.93.184434.

H. B. G. Casimir. On the attraction between two perfectly conducting plates. *Proceedings of the Koninklijke Nederlandse Akademie van Wetenschappen*, 51:793–795, 1948. URL https://dwc.knaw.nl/DL/publications/PU00018547.pdf. Original Proceedings reprint PDF hosted by KNAW.

R. S. Decca, D. López, E. Fischbach, G. L. Klimchitskaya, D. E. Krause, and V. M. Mostepanenko. Precise comparison of theory and new experiment for the casimir force leads to stronger constraints on thermal quantum effects and long-range interactions. *Annals of Physics*, 318(1):37–80, 2005. doi: 10.1016/j.aop.2005.03.007. URL https://doi.org/10.1016/j.aop.2005.03.007.

S. K. Lamoreaux. Demonstration of the casimir force in the 0.6 to 6 μm range. *Physical Review Letters*, 78(1):5–8, 1997. doi: 10.1103/PhysRevLett.78.5. URL https://doi.org/10.1103/PhysRevLett.78.5. Erratum: Phys. Rev. Lett. 81, 5475 (1998), doi:10.1103/PhysRevLett.81.5475.

A. O. Sushkov, W. J. Kim, D. A. R. Dalvit, and S. K. Lamoreaux. New experimental limits on non-newtonian forces in the micrometer range. *Physical Review Letters*, 107(17):171101, 2011. doi: 10.1103/PhysRevLett.107.171101. URL https://doi.org/10.1103/PhysRevLett.107.171101.

David W. Thomson III. Casimir–nuclear chronovibration as the cosmological driver: A full qmu derivation. QADI working paper (PDF); also posted as Zenodo Preprint, 2025a. URL https://doi.org/10.5281/zenodo.17498321. QMU-native derivation and cosmological application.

David W. Thomson III. Casimir-driven aether nucleation and matter creation in qmu, September 2025b. URL https://doi.org/10.5281/zenodo.17194030. Version v1, published 2025-09-24.

David W. Thomson III. A topological origin for cosmic birefringence: A parameter-free prediction of $\beta_0 = 1/(16\pi^2)$. QADI working paper (PDF)also posted as Zenodo Preprint, 2025c. URL https://doi.org/10.5281/zenodo.17069938. Topology-based prediction of the universal $1/(16\pi^2)$ factor.

David W. Thomson III. A novel interpretation of the photoelectric effect using the aether physics model. QADI working paper (PDF); also posted as ResearchGate Preprint, 2025d. URL https://doi.org/10.13140/RG.2.2.11217.95848. APM/QMU interpretation of photoelectric threshold and emission mechanics.

David W. Thomson III and James D. Bourassa. A unified force theory based on quantum aether dynamics: Predictions and experimental support. QADI working paper (PDF); also posted as Preprints 2024, 2024090007 (v1), 2025. URL https://doi.org/10.20944/preprints202409.0007.v1. Preprints v1 posted 2024-09-02.